Procedings of COBEM 2005
18th International Congress of Mechanical Engineering
November 6-11, 2005, Ouro Preto, MG

A NUMERICAL INVESTIGATION ON TRANSIENT WAVE PROPAGATION PHENOMENA AT 2D HALF-SPACES AND THE TRANSIENT RESPONSE OF RIGID SURFACE FOUNDATIONS

Luiz Henrique Thomazo
Dept. of Computational Mechanics - DMC/FEM
State University at Campinas - UNICAMP, Brazil
luth@fem.unicamp.br

Euclides Mesquita
Dept. of Computational Mechanics - DMC/FEM
State University at Campinas - UNICAMP, Brazil
euclides@fem.unicamp.br

Abstract. *The Boundary Element Method (BEM) is an efficient numerical tool to describe the dynamics of rigid bodies interacting with unbounded domains, in which the Sommerfeld radiation condition plays an essential role. For transient analysis the synthesis of the Boundary Integral Equations (BIE), which forms the basis of the BEM, requires an auxiliary transient state. This auxiliary state is usually a transient stress boundary value problem of the elastodynamic.*

In the present article two distinct auxiliary states are used to synthesize the BIE governing the transient response of rigid foundations. These auxiliary states represent the solution of a stress boundary value problem. The spatial stress boundary condition for both auxiliary cases is a constant load with a prescribed width applied at the half-space surface. The time variation of the applied stress boundary conditions are, respectively, a Dirac's Delta function and a Heaviside function.

The wave propagation patterns generated at the half-space surface by these two distinct time load functions are investigated. An analysis of the transient wave propagation phenomena at the half-space indicates that surface loads containing traction discontinuities generate dilatational, shear and Rayleigh waves at every load discontinuity. These multiple wave fronts impinge, at proper time instants, the surface points at which foundation kinematic compatibility is prescribed leading to abrupt oscillations in the foundation transient response. In this article the interaction of the wave propagation pattern, generated by both auxiliary solutions, with the transient rigid foundation response will be investigated.

Keywords: *Boundary Element Method, Transient response, Foundation dynamics, Wave propagation*

1. Introduction

In a previous article (Mesquita et al., 2004) the authors of the present work have shown that the transient response of a 2D rigid foundation interacting with a soil, modelled as a viscoelastic half-space, presented a series of peaks. These peaks were shown to be related to the Rayleigh wave front propagation at the soil-foundation interface. When these wave fronts arrive at the interface points used to establish rigid body kinematic compatibility, they produced the mentioned response peaks.

On the other hand, other Boundary Element researchers claim that using a Heaviside excitation function, such peaks or oscillations were not captured at the transient response. Now the issue is raised, whether these peaks are present or not in the rigid foundation response due to the Heaviside function excitation. The present paper investigates this issue. It will compare the solution obtained by both approaches, correlate them to the wave propagation pattern at the soil-foundation interface and furnish an explanation for the occuring phenomena.

2. Statement of the Stationary Problem

The stationary stress boundary value problems (SBVP) being addressed is governed by the Navier differential equation of a linear viscoeastic continua, which can be expressed in terms of the displacement components $\overline{u}_i$:

$$\mu^* (\omega) \cdot \overline{u}_{i,jj} + [\lambda^* (\omega) + \mu^* (\omega)] \cdot \overline{u}_{j,ji} + \rho\omega^2 \overline{u}_i + f_i = 0 \tag{1}$$

In Equation (1) the circular frequency is ω, the continuum density is ρ and f_i are the components of the body forces.

The quantities μ^* and λ^* are complex Lame's constants. These constants are responsible for the insertion of the viscoelaticity through of the correspondence principle (Christensen, 1982). The constants are defined by $\mu^* [1 + i\eta(\omega)]$ and $\lambda^* [1 + i\eta(\omega)]$, with η being the damping factor. The boundary conditions, determining the half-space auxiliary state, consists of a vertical constant traction distribution applied at the half-space surface Γ^S, shown in Figure (1), and described by:

$$t_z(x,z=0) = \begin{cases} t_z & \text{if } |x| \leqslant a, \\ 0 & \text{if } |x| > a. \end{cases} \tag{2}$$

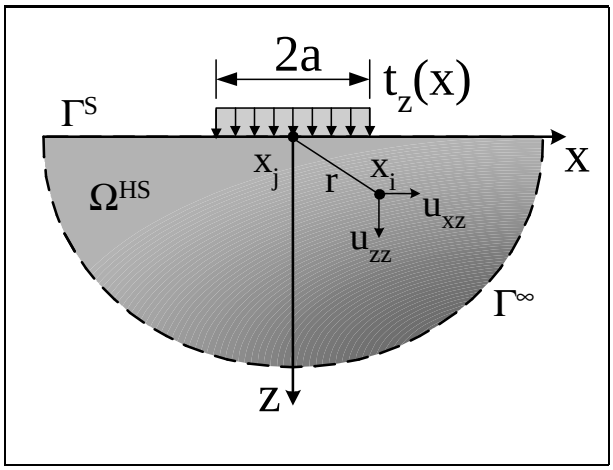

Figure 1. State Auxiliar - 2D

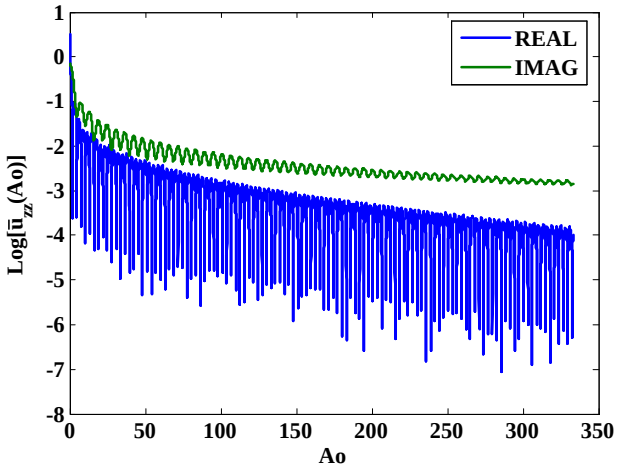

Figure 2. Displacement solution in the frequency domain.

2.1 Solution of the Stationary Auxiliary State

The stationary problem, described by boundary value problem, is solved with the aid of the Fourier Integral Transform. The inverse transform is computed numerically. The typical solutions for displacements u_i and stresses σ_{ij} may be found in Barros and Mesquita, (1999). A strategy based on the Longman, (1956) algorithm for improper integration, combined with an adaptive quadrature scheme (Forsythe, 1977) was developed to perform the numerical integrations with the following structure:

$$\overline{u}_{ij}(x_p,x_q,z,\omega) = \int_{-\infty}^{+\infty} \overline{H}_{ij}(x_p,x_q,z,\omega,k,\rho,\lambda,\mu,\eta)\, \overline{t}_j(x_q,k)\, e^{ixk} dk \tag{3}$$

In Equation (3) $\overline{u}_{ij}(x_i,x_j,z,\omega)$ are the displacements at a point x_i displacements at the half-space, due to loaded area with center at x_j,(see fig.1). $H_{ij}(x_i, x_j, z, \omega, k, \rho, \lambda, \mu, \eta)$ is the kernel of the stationary viscoelastic solution to be found in Barros and Mesquita, (1999) and $t_j(x,k)$ are the surface tractions in j-th direction, written in the wave number domain k.

In Figure (2) is possible see the Log_{10} a typical displacement solution for the stationary case, as a function of the dimensionless frequency parameter is $Ao = \frac{\omega a}{c_s}$, in which a is the load half-width and $c_s = \sqrt{\frac{G}{\rho}}$ is the shear wave velocity of the elastic continuum, G is the shear modulus and ρ is the density. An analysis of Figure (2) shows that the implemented integration strategy is able to synthesized stable numerical solutions at very high frequencies. It should be stressed that for most engineering applications the analysis is limited to low frequencies $Ao < 10$ (Gazetas, 1983). The high frequency results are determined to ensure transient responses with very short time steps (Mesquita et al., 2002).

3. Solution of the Transient Auxiliary State.

The transient solutions are obtained by applying the Fast Fourier Algorithm (FFT) with respect to the pair (ω, t) or (Ao, t) to the previously synthesized frequency domain solutions. One important issue in the discrete FT is the relation between the k-th frequency step $\Delta Ao = Ao_{k+1} - Ao_k$ and the maximum time reachable by the transient process, $Tmax$,

$\Delta Ao = \frac{2\pi}{Tmax}$ and the relation between the time step Δt and the maximum sampling frequency $Aomax$, $\Delta t = \frac{2\pi}{Aomax}$. This implies that for very small time steps Δt the maximum sampling frequency $Aomax$ must be high. Prior to obtaining stable transient results, the stationary signal must undergo a mathematical treatment, as described in Mesquita et al., (2002).

3.1 Transient response due to a Dirac's Delta time loading.

Figure (3) depicts a series of transient responses obtained at different locations x_i at the half-space surface. The spatial loading is a constant vertical traction t_z with width $2a$. The load time dependance is a Dirac's Delta applied at the initial instant $f(t) = \delta(t = 0)$. The parameters for the given solution are: $G = 1\ [N/m^2]$, Poisson ration $\nu = 0{,}333$, density $\rho = 1\ [kg/m^3]$. The damping is considered to be constant hysteretic with parameter value $\eta = 0{,}01$. Under these conditions the dilatational, shear and Rayleigh wave velocities are, respectively $c_p = 2{,}0\ [m/s]$, $c_s = 1{,}0\ [m/s]$ and $c_R = 0{,}932\ [m/s]$.

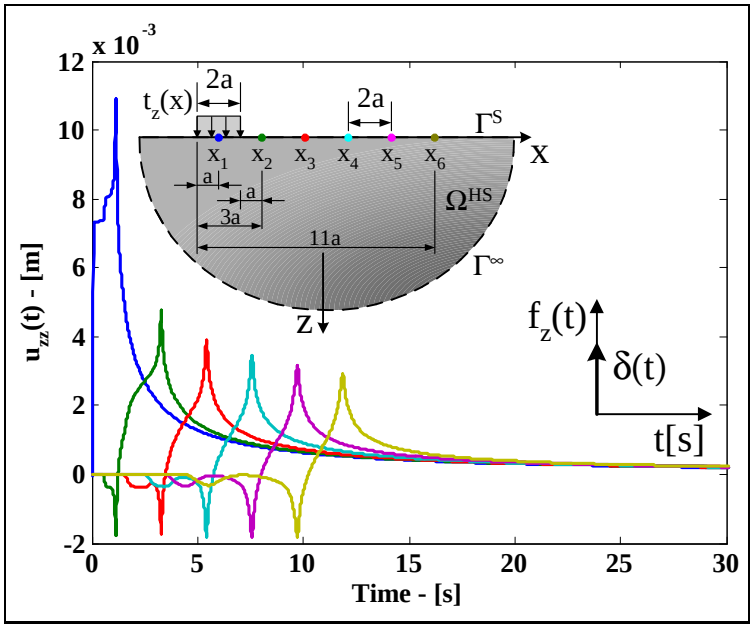

Figure 3. Solution of the Transient State Auxiliar in Surface (Excitation Dirac's Delta).

Figure (3) reveals clearly the arrival times of the body (c_S, c_p) and surface wave (c_R) impinging the different measure stations x_i ($i = 1$,,6). These wave fronts were originated at the stress discontinuities of the load at $x = -a$ and $x = +a$.

A detailed displacement response $u_{zz}(t)$ - vertical displacement due to vertical loading - at the point $x_1 = 0$ for the initial time instants can be viewed at Figure (4). It can be observed that the reponse consists of an initial displacement occuring with velocity c_p, followed by a nearly constant displacement. After $t = 0{,}5s$ the dilatational waves (c_p) stemming from the stress discontinuities at $x = \pm a$ arrive at $x_1 = 0$. The arrival of the wave front is clearly visible. After the arrival of the wave front, a continuous contribution from the loading extending in the unlimited y direction is added to the displacement. This is a typical result for a plane state of strain.

The arrival of the shear (c_s) and Rayleigh (c_R) wave fronts are visible around the time instant $t = 1s$. The shear and wave front produce a large peak in the surface displacement. This response peak will influence decesively the rigid foundation response, as will be shown later. After the shear and Rayleigh wave fronts have passed by the measuring point $x_1 = 0$, the solution decays monotonically towards the initial state of equilíbrium. This monotonic fall, also called the "solution tail" is also typical for the plane strain solution. It indicates that the wave fronts are no longer present, but that there are contributions from the continuous load extending in the unlimited $y - direction$. This effect is shown in Figure (5), which shows that the plane strain case extends indefinitely in the $y - direction$.

3.2 Transient response due to a Heaviside time loading.

Figures (3) and (4) furnished the transiente solution for the case of a Dirac's Delta time loading. Now the transient response due to a Heaviside time loading will be investigated. The authors of this article concluded that, in order to investigate the response to the Heaviside time loading, the response to a series of "windows of constant amplitude", should be addressed.

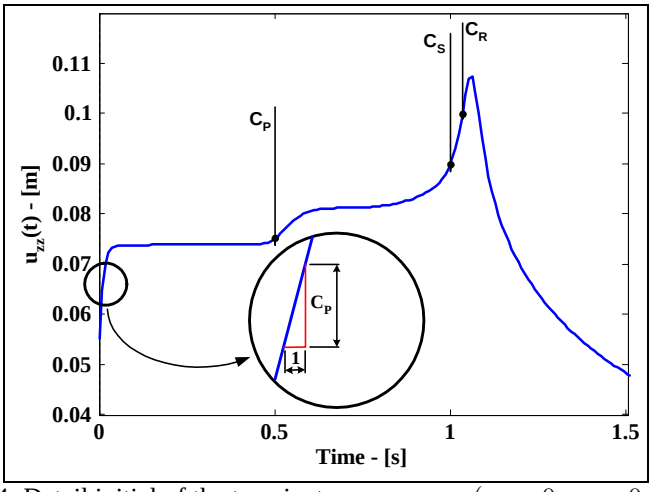

Figure 4. Detail initial of the transient response $u_{zz}\,(x_i = 0, x_j = 0, z = 0)$.

The window loading was constructed by adding and subtracting the Heaviside function $H\,(t)$ at an intervalΔt. The load window is given by $f_w\,(t, \Delta t) = +H\,(t - 0) - H\,(t - \Delta t)$. The vertical transient response $u_{zz}\,(t, \Delta t)$ due to a window loading with $\Delta t = 0{,}464s$ is shown in Figure (6). The measuring point is the origin $x_1 = 0$. Compared to the solution for the Dirac excitation given in Figure (3), it can be seen that this response is smoother than the former. This can be physically explained. Actually the response to a window time loading is a sum, in integral sense, of a series of Diracs solutions. The summation of multiple wave fronts tend to smooth the original sharp wave fronts.

It should be mentioned that the time length of the window producing the result in Figure (6) is smaller than the time the dilatational wave requires to cover the distance from the load discontinuities at $x = \pm a$ to the origin ($t_P = a/c_p = 0{,}5s$).

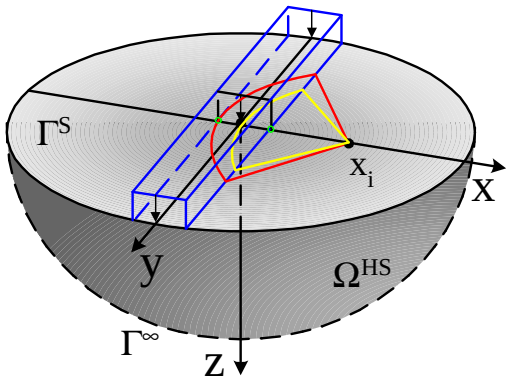

Figure 5. Representation of the problem 2D in scheme 3D.

Now it is interesteing to investigate the effect produced by increasing the window length (Δt) continuously. Figure (7) shows the transient displacement response u_{zz} for distinct values of the time windows length ($\Delta t = 0{,}464s$, $0{,}928s$, $1{,}392s$, $2.321s$). This windows were chosen so that each one finished short before one of the wave fronts would arrive at the origin $x_1 = 0$. Considering that for each window the momentum introduced by the excitation increases linearly and

that the corresponding maximum displacement also increases according to the same rule, the displacements in Figure (7) were all normalized by their maximum values.

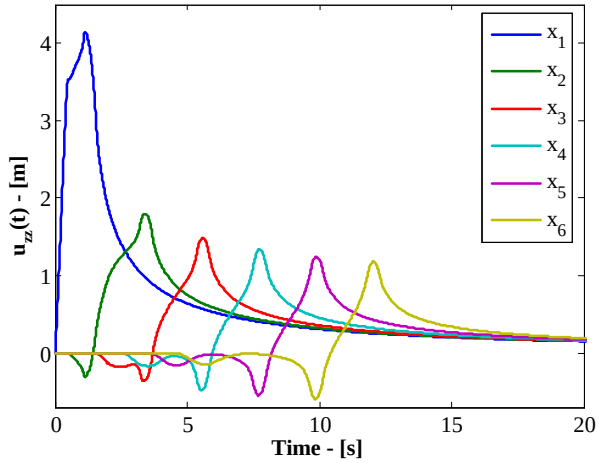

Figure 6. Detail initial of the transient response in surface $u_{zz}\,(x_i, x_j = 0, z = 0)$ - Constant window $\Delta t = 0{,}464\ [s]$.

The key issue in this article is given by the displacement solutions shown in Figure (7). These solutions point out clearly that displacements due to the stress loading (the constant spatial loading applied continuously during the time window) surpass largely the displacements originated by the arrival of the wave fronts. The displacement changes due to the arrival of the body and surface waves, which were very clear at the Dirac's time excitation solution, are overshadowed by displacements caused by the stress distributions. As the window increases and encompasses the arrival times of the body and surface waves, their contribution is smoothed.

The smoothing of the peaks, originally produced by the arrival of the body and surface waves, due to a window time excitation or due to a Heaviside time loading, will have a significant effect on the transient response of the rigid foundations interacting with the soil.

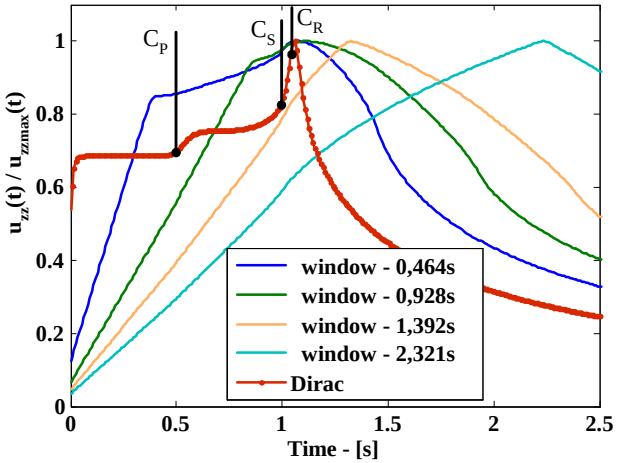

Figure 7. Detail initial of the transient response $[u_{zz}/u_{zzmax}]\,(x_i = 0, x_j = 0, z = 0)$ - Heaveside's Excitations.

4. Rigid Foundation Response

The solution of the body rigid is based on the superposition of the auxiliary states for loads distributed at the half-space surface, considering rigid body kinematic compatibility condition and force equilibrium at the soil-foundation interface. The analysis is carried in the frequency domain. Thus, three elements are necessary to determine the rigid foundation

response. The first element is a stationary displacement solution at the half-space surface. In the sequence the soil-foundation interface is divided in "n" constant (elements). The total displacement solution at a point x_i is give by the superposition of the "n" constant loads with intensity t_r acting at the soil-foundation interface as show in Figure (8). The displacement may be writter as:

$$\{\overline{u}_p\,(x_i,\omega)\} = \frac{1}{\pi\mu}\left[H_{pr}\,(x_i,x_j,z,\omega,k,\rho,\lambda,\mu,\eta)\right]\{t_r\,(x_j,k)\} \tag{4}$$

with "i" being the response, point "j" is the point a which the load is applied and (p,r) are, respectively, the response and load direction. The second element is the equilibrium among the vector or external loading acting on the foundation $\{Fe\}$ and the soil reactions $\{t_r\}$.

$$\{Fe\} = [E_Q]\,\{t_r\} \tag{5}$$

The last element is the kinematic compatibility equations, relating the total displacements u_{ij} at nodes "i", with the rigid foundation degrees of freedom $\{u_f\} = \{u_{zf}, u_{xf}, \varphi_{yf}\ A\}^T$:

$$\{u_{ij}\} = [C_c]\,\{u_f\} \tag{6}$$

A very important issue regarding the kinematic compatibility conditions is the fact that it is a "point-wise" compatibility condition. This assumption will have a significant influence on the rigid foundation transient displacement response. Equations (4), (5) and (6) can be combined to yield the following equation system:

$$\begin{bmatrix} \frac{1}{\pi\mu}H_{pr} & -C_C \\ E_Q & 0 \end{bmatrix}\begin{Bmatrix} t_r \\ u_f \end{Bmatrix} = \begin{Bmatrix} 0 \\ Fe \end{Bmatrix} \tag{7}$$

In the system indicated by Equation (7) it is possible to determine the soil-foundation interface tractions $\{t_r\,(t)\}$ and the rigid foundation transient response $\{u_f\,(t)\}$ due to a transient external excitation $\{Fe\,(t)\}$.

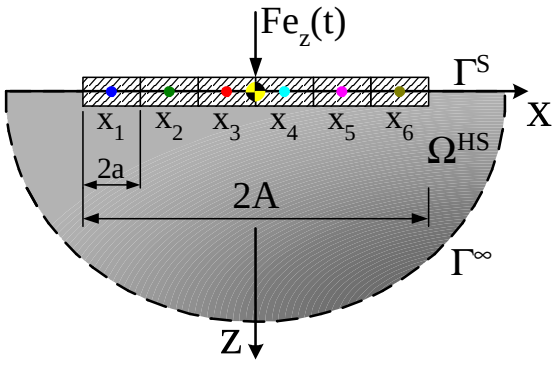

Figure 8. Foundation rigid in half-space.

The described methodology was applied to determine the response of a rigid foundation interacting with the half-space. The soil foundation interface was divided into 6 constant elements, as indicated in Figure (8).

Initially the response due to a Dirac's Delta excitation was determined. In the sequence the response to a series of increasing time windows was obtained. Figure (9) shows the calculated results. The transient response due to a Dirac's time loading presented a series of peaks. The origin and meaning of these peaks have already been explained by Mesquita et al., (2004). These peaks correspond to the arrival of the Rayleigh wave fronts at the soil-foundation interface points that were used to establish rigid body kinematic compatibility equations.

On the other hand, as the excitation window time increases the influence of the displacement wave fronts are smoothed and the peaks in the transient foundation response tend to disappear. This effect is clearly depicted in Figure (9). So, it has been shown that the use of windows or Heaviside time loadings eliminate gradually the oscillations present in the rigid foundation response in the case of a Dirac's time loading.

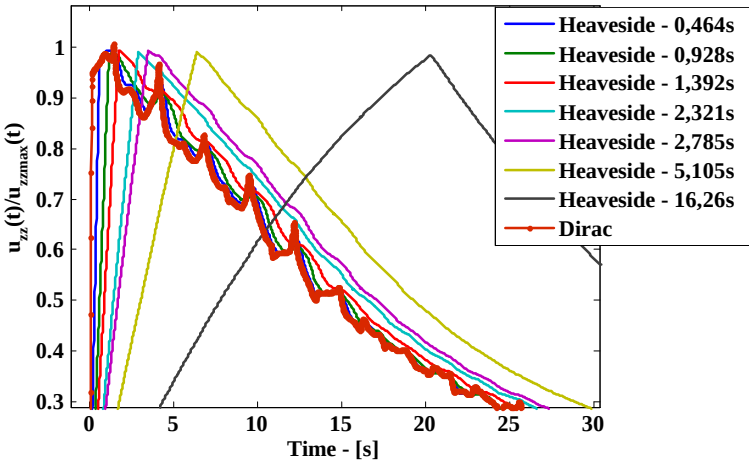

Figure 9. Detail initial of the transient response of the body rigid $[u_{zz}/u_{zzmax}]$ $(x_i, x_j = 0, z = 0)$ - Heaveside's Excitations.

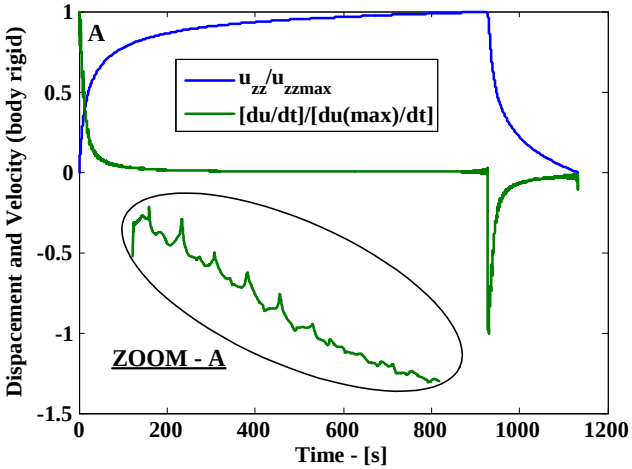

Figure 10. The transient response of the body rigid (displacement and velocity) $(x_i, x_j = 0, z = 0)$ - Heaveside's Excitations - 928 $[s]$.

The normalized transient solution $u_{zz}(t)/u_{zzmax}$ for a very large time window, tending to the Heaviside function, is shown in Figure (10). The time derivative of this solution is also presented. It can be seen that the transient rigid foundation response to the Heaviside function is very stable and consistent. The derivative of the Heaviside solution should reproduce the solution due to the Dirac's excitation. This is also shown, correctly in Figure (10). A magnification of the derivative of the Heaviside response for the initial time instants (zoom) is shown in the lower part of the picture. The presence of the peaks in the response obtained by numerical derivation of the Heaviside solution, indicate that the procedure presented in this article is consistent.

5. Concluding Remarks

In this article the transient response of two-dimensional rigid foundation interacting with a half-space has been analyzed. The transient response was obtained by superposing two distinct auxiliary states. The first auxiliary state was obtained by solving a stress boundary value problem with constant spatial load distribution and a Dirac's time excitation loading. The second auxiliary state is synthesized by appliying a window of constant time loading. This window was increased in length simulating a Heaviside function. A comparison between the response due to a Dirac's Delta excitation and a Heaviside function allows to explain the origin of the peaks in the Dirac's solution. Furthermore it has been shown that the Heaviside load smoothes the transient response peaks. The authors believe this to be an original research result.

6. Acknowledgements

This research has been supported, throughout the years, by the following funding agencies: Fapesp, CNPq, Capes and FAEP/UNICAMP. This is greatfully acknowledged.

7. References

Barros, P. L. A. and Mesquita, E. N. (1999). Elastodynamics Green's functions for orthotropic plane strain continua with inclined axis of symmetry. *International Journal for Solids and Structures*, 36:4767–4788.

Christensen, R. M. (1982). *Theory of Viscoelasticity.* Academic Press, New York.

Forsythe, G. E. (1977). *Computer Methods for Mathematical Computations.* Prentice Hall.

Gazetas, G. (1983). Analysis of machine foundation vibrations: State of the art. *Soil Dynamics and Earthquake Engineering*, 2:2–42.

Longman, I. M. (1956). Note on method for computing infinite integrals of oscillatory functions. volume 52, pages 764–768.

Mesquita, E. N., Adolph, M., Barros, P. L. A., and Romanini, E. (2002). Transient Green and influence functions for plane strain visco-elastic half-spaces. In *IABEM 2002 (Internation Association for Boundary Element Methods)*, pages 1–12, The University of Texas at Austin, Texas, USA.

Mesquita, E. N., Thomazo, L. H., and Barros, P. L. A. (2004). On the transient wave propagation phenomena at 2d half-space surfaces and rigid foundations response. In *5th International Conference on Boundary Element Techniques, Lisboa, Advances in Boundary Element Techniques V. UK : EC Ltd.*, volume 1, pages 39–44, Lisboa.

8. Responsibility Notice

The authors are the only responsible for the printed material included in this paper